electronics

MDPI

Article

Distributed Integrated Energy System Optimization Method Based on Stackelberg Game

Mao Yang [1], Weining Tang [1,2], Jianbin Li [1] and Peng Sun [1,*]

[1] Key Laboratory of Modern Power System Simulation and Control & Renewable Energy Technology, Ministry of Education (Northeast Electric Power University), Jilin City 132013, China
[2] State Grid Jilin Electric Power Co., Ltd., Songyuan Power Supply Company, Songyuan 132013, China
* Correspondence: sunpeng@neepu.edu.cn

Abstract

As the composition of energy markets becomes increasingly diverse and distributed in character, it is difficult for traditional vertically integrated energy system (IES) structures and centralized optimization methods to stimulate coupled interactions and interactive synergies among multiple subjects. Consequently, a collaborative low-carbon scheduling strategy utilizing a leader–follower game framework is introduced for the distributed IES. Making the integrated energy system operator (IESO) a leader, distributed integrated energy supply system (DIESS) and smart user terminal (SUT) as followers, the optimal interaction operation strategy of each subject in the game process can be solved. Firstly, the overall energy interaction process of the system and the game objectives of each participant are introduced to construct a distributed collaborative optimization model with one leader and multiple followers. Secondly, the integrated demand response (IDR) and the ladder-type carbon trading scheme are considered, the two-stage operation process of the electrical gas technology (P_2G) equipment is analyzed in detail, and the genetic algorithm nested CPLEX solver is used to solve the model. Finally, the results show that this paper can provide guarantee and theoretical support for the optimal operation of the integrated energy market in terms of trading model and algorithm.

Keywords: Income distribution; dynamic pricing; Stackelberg game; integrated demand response; carbon trading

1. Introduction

In current times, with the accelerated evolution of the IES sector, their heterogeneous and decentralized nature has become more and more obvious. Energy is transforming into distributed renewable energy use, and the new energy system that combines renewable energy technology and internet technology, energy internet, is developing rapidly, which is also the main direction and objective requirement for the development of comprehensive energy system innovation [1]. Research focus has increasingly shifted towards IES frameworks centered on the DIESS, which are characterized by the integration of source, network, and load elements. It facilitates the widespread deployment of new energy sources, realizes the complementary advantages of different energy sources, and ensures the economic and efficient use of energy within the system [2–4]. However, the primary challenge in current low-carbon transitions lies in the inherent conflict between rigid policy constraints, such as ladder-type carbon trading, and the decentralized flexibility of diverse energy prosumers. How to effectively guide these heterogeneous agents to synchronize their behaviors with

Check for updates

Academic Editor: Spyridon Nikolaidis

Received: 13 January 2026
Revised: 3 February 2026
Accepted: 4 February 2026
Published: 7 February 2026

Copyright: © 2026 by the authors. Licensee MDPI, Basel, Switzerland. This article is an open access article distributed under the terms and conditions of the Creative Commons Attribution (CC BY) license.

systemic decarbonization targets under non-smooth price signals remains an urgent yet under-explored motivation.

According to the different optimization models established, they can be divided into centralized integrated energy systems and distributed integrated energy systems, and the current domestic and international research on integrated energy systems mainly focuses on centralized optimized operation strategies [5]. Refs. [6–8], study DIESS multi-objective optimization operation strategies for different structures. Ref. [9] investigates individual DIESS energy supply operation and clustered DIESS energy supply operation; however, the aforementioned articles only focus on the energy supply side, ignoring the information interaction between the energy networks of distributed integrated energy systems and the autonomy of the load side. Ref. [10] provides a review of the concept, framework, and model of the IDR, reviews the current state of research on the optimal operation and solution methods for the IDR, and explores the market mechanisms and business models for the IDR. Refs. [11,12] investigate the optimal operation strategy of integrated energy systems considering load side IDR. Refs. [13,14], investigate the role of the IDR in the face of clustered loads and show that IDR can achieve a flattening of the load profile and improve system operational stability while reducing energy costs.

The above study effectively improves the system economy and stimulates the flexibility of the load side by building different optimization models. If the information flow in the energy network can be used wisely, it will definitely contribute to the optimal scheduling of the system [15]. For example, energy prices not only influence the energy use behavior on the load side, but the energy demand on the load side can also counteract the setting of energy prices, and the implementation of this strategy requires the use of information flow.

The distributed optimization of IES aligns more closely with the operational characteristics of the contemporary energy market, for example, game theory [16,17], alternating direction multiplier method [18], consistency theory [19], etc. For distributed IES, it is very appropriate to choose game theory to solve this problem because it involves information interaction and conflict of interests among multiple market players. Nevertheless, these game-theoretic models typically assume continuous and differentiable cost functions, overlooking the policy-induced non-smoothness that can trigger numerical instability and reshape the Nash equilibrium. Refs. [20–22] use game theory to achieve interactive operational strategy formulation among various market players and to develop dynamic energy prices through information flow in energy networks to achieve the interest goals of game participants. Ref. [23] proposes a future pricing and power purchase strategy for intelligent cell agents, modeling the agent's and owner's respective pursuit of interest maximization as a master–slave game. Ref. [24] points out that robust optimization is currently difficult to combine effectively with Stackelberg game theory. In Ref. [25], a cooperative game allocation model was developed to solve the benefit distribution problem among the game participants. In Refs. [26–28], it is indicated that the dual-clustering PV forecasting framework, combined with the equivalent wind power curve technique, can significantly enhance wind power prediction precision and offer superior support for optimal scheduling.

To protect the atmosphere and reduce carbon footprints, low carbonicity is also a hot issue in the field of IES. In Refs. [29–31], a ladder-type carbon trading scheme is used to improve the low-carbon nature of the infrastructure, which is more conducive to reducing system carbon footprints than traditional carbon trading, and also reduces system operating costs. In Ref. [32], the authors explore the diverse advantages of hydrogen energy by elaborating on the dual-stage P_2G operation, which incorporates an electrolyzer, a methane reactor, and a hydrogen fuel cell. Moreover, existing studies on ladder-type mechanisms often adopt a centralized optimization perspective, which fails to capture the

dynamic cost–transmission laws among competitive agents or the role of P_2G as a strategic buffer in a decentralized game loop. The specific comparison is shown in Table 1.

Table 1. Comparison of the literature.

	Multi-Agent Stackelberg Game	Ladder-Type Carbon Trading	Two-Stage Refined P_2G	Handling of Non-Smooth "Kinks"	Behavioral Coupling Analysis
[16,17,19,20]	Yes	Yes	Partial	No	No
[29–31]	No	Yes	No	No	No
[32]	No	No	Yes	No	No
body of the work	Yes	Yes	Yes	Yes	Yes

To fill these gaps, this paper moves beyond the modular aggregation of existing tools by exploring the inter-subject behavioral coupling within a multi-agent game specifically under non-smooth carbon signals. The core research gap we address is the lack of a robust methodology that can reconcile the mathematical non-convexity of bi-level gaming with the non-smoothness of progressive carbon penalties.

In light of the aforementioned context, the present work investigates a decentralized collaborative optimization approach within a Stackelberg game framework. A master–slave game model with the IESO as the leader and the DIESS and SUT as the followers is constructed, and the corresponding mathematical model is given to optimize the pricing strategy of the IESO, the energy supply plan of the DIESS, and the energy demand of the SUT at the same time. The energy trading process is introduced and solved using a genetic algorithm nested with a CPLEX solver (v22.1, IBM Corp., Armonk, NY, USA). Finally, the efficacy of the developed optimization framework in terms of operational enhancements at both the generation and consumption ends is verified through the analysis of calculation cases. Moving beyond the modular aggregation of existing optimization tools, this study explores the inter-subject behavioral coupling and the redistribution of carbon abatement responsibilities within a multi-agent game. The primary contributions are summarized as follows:

(1) The dynamic transmission law of carbon cost in a multi-agent game is revealed. Different from previous studies that attribute carbon emission responsibility to a single subject, we deeply discuss how the ladder-type carbon trading scheme transmits the cost signal of low-carbon transformation to the supply side and the demand side in real time through IESO's pricing leverage. Through this model, we can observe how the carbon price signal induces DIESS and SUT to change their original operating inertia, which provides a new perspective for understanding the role of the carbon market in a multi-energy coupling environment.

(2) Formulating a low-carbon coupling dispatch strategy based on refined P_2G modeling. We have introduced a two-stage P_2G carbon reduction process and integrated it deeply with the ladder-type carbon trading mechanism. Our simulation analysis reveals that within a game environment, P_2G acts not only as a tool for energy conversion but also as a "buffer" that regulates the pricing elasticity of the entire system. This refined modeling approach uncovers the non-linear evolutionary relationship between energy conversion efficiency and economic returns across different carbon price intervals, offering a more operational scheme for the low-carbon scheduling of IES.

(3) Designing and validating a hybrid optimization framework that balances computational efficiency and solution quality. Given the complex mathematical features of the leader–follower game model—such as non-convexity, non-smoothness, and discrete variables—we have designed a GA–CPLEX hybrid solution scheme. By strategically partitioning the responsibilities between external pricing searches and

internal linear programming, this framework effectively avoids the pitfalls of local optima common in pure heuristic algorithms while ensuring the uniqueness and rigor of the followers' responses in each iteration. Comparative experiments across multiple scenarios demonstrate the superiority of this scheme in handling complex bi-level optimization problems.

2. Distributed Integrated Energy System Frame

The integrated energy system proposed in this paper consists of three parts: IESO, DIESS, and SUT. Based on the DIESS, the IESO functions as a critical interface linking the upstream energy network with the SUT, thereby facilitating cost-effective, low-carbon power provision and promoting rational energy. A detailed architecture design is depicted in Figure 1.

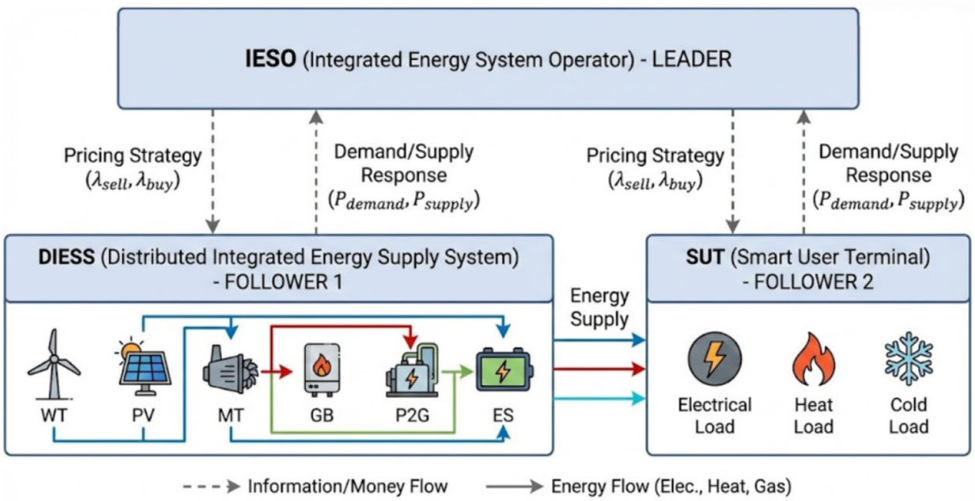


Figure 1. Schematic diagram of the game subject framework of the distributed integrated energy system.

2.1. Structure of Integrated Energy System Operator

The tripartite game of distributed integrated energy system is shown in Figure 2. The IESO considers trading of electricity, heat, and cold energy, and makes the energy price by aggregating the decision information provided by the DIESS and the SUT. The overall system realizes the tripartite game through the link of energy price and gains from it. Introducing the IESO as a market player in IES energy interaction and strategy formulation can stimulate the DIESS to participate in energy market competition and encourage the SUT to develop in the direction of scientific and rational energy use. In the energy trading process, the IESO also needs to bear the risk caused by energy price fluctuations, and supply and demand imbalances. When the output power of the DIESS cannot reach the load side energy demand, the IESO needs to purchase energy from the higher energy network at a high price to make up for the power gap. If the power gap still cannot be filled, it needs to pay the corresponding penalty fee. Therefore, developing a reasonable and optimal scheduling strategy is a practical guarantee that the IESO can earn revenue.

2.2. Structure of the Distributed Integrated Energy Supply System

The DIESS complements the advantages of renewable energy and traditional fossil energy to provide energy support for the SUT. Among them, renewable energy generation mainly includes wind power and photovoltaic power. The coupling equipment includes a cogeneration unit consisting of a micro turbine (MT) and a heat recovery steam generator (HRSG) to provide electrical and heat energy to the system; the gas fired boiler (GB) consumes natural gas to produce heat, the electric boiler (EB) consumes electrical energy to

provide heat for the system. The electric chiller (EC) is powered by electricity, whereas the absorption chiller (AC) utilizes thermal energy to serve as the cooling load.

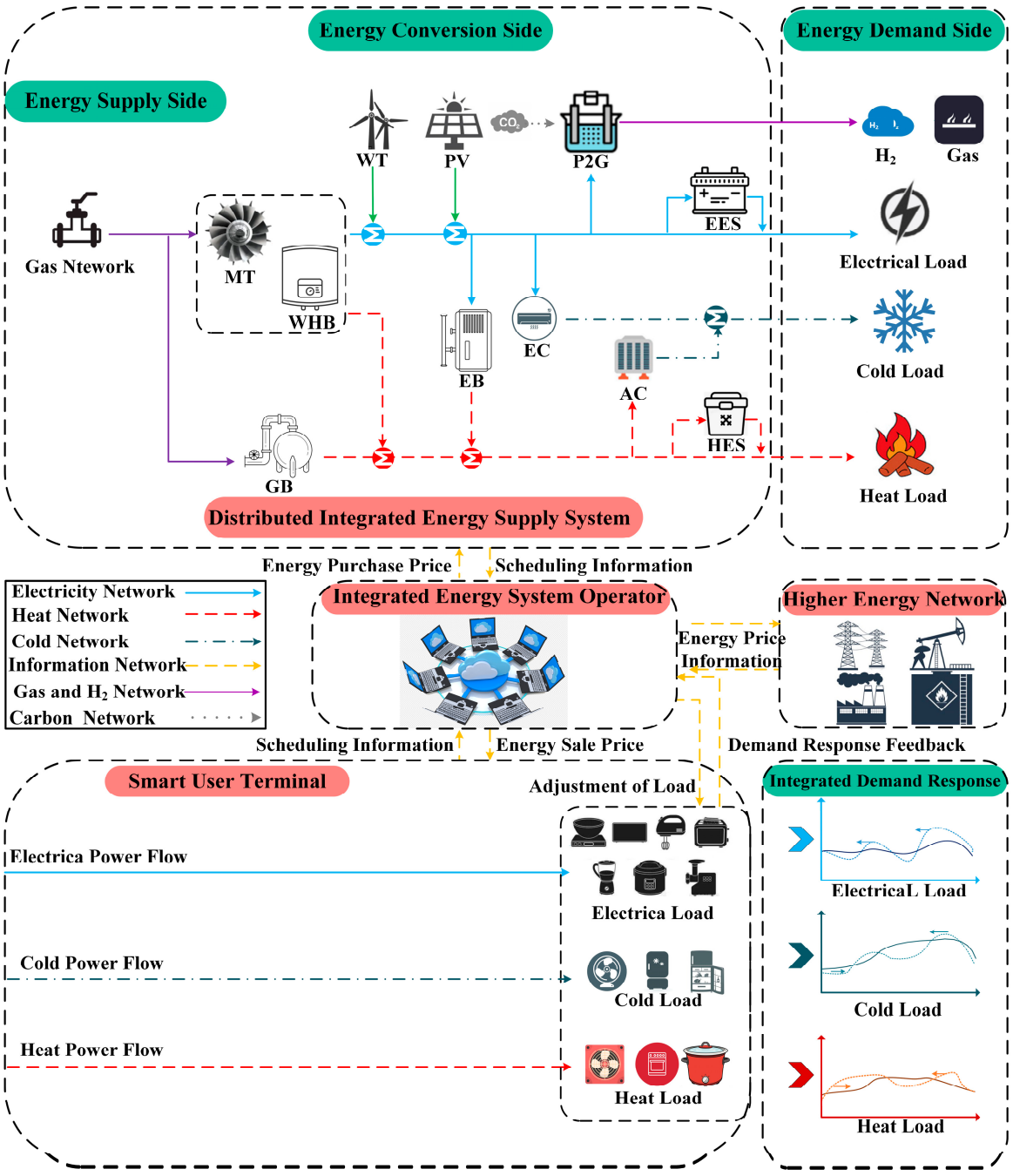


Figure 2. Diagram of the tripartite game of distributed integrated energy system.

When wind turbine (WT) or photovoltaic (PV) power generation is abundant, P_2G equipment can convert excess electricity into natural gas energy and reduce carbon footprints. Storage devices encompass electric energy storage (EES), and heat energy storage (HES), which are responsible for storing energy and calming the load. The DIESS optimizes the time-to-time output of each equipment in the system through the pricing signals determined by the IESO with the aim of enhancing its financial returns.

2.3. Structure of the Smart User Terminal

The SUT consolidates diverse energy load requirements within the framework, participates in energy interaction on behalf of the user body, and accepts supervision. Due to the multi-energy coupling characteristics of the IES, this paper considers the IDR to subdivide the load into the fixed load, curtailable load, and transferable load. The SUT makes adjustments to the user's energy consumption behavior by receiving the energy price information provided by the IESO. The above diagram of the information interaction and energy trading between the IESO, DIESS, and SUT is shown in Figure 2.

3. Distributed Integrated Energy System Model

3.1. Integrated Energy System Operator Model

The IESO considers the energy input on the supply side and the energy output demand on the demand side and sets energy prices with the goal of maximizing its profitability, which can be expressed as the following function:

$$\max F_{IESO} = \sum_{m=1}^{M}\sum_{t=1}^{T}\left(C_{sell,m}^{t} - C_{buy,m}^{t} - C_{net,m}^{t} - C_{pun,m}^{t}\right) \tag{1}$$

$$C_{sell,m}^{t} = P_{load,m}^{t} c_{sell,m}^{t} \Delta t \tag{2}$$

$$C_{buy,m}^{t} = P_{pro,m}^{t} c_{buy,m}^{t} \Delta t \tag{3}$$

$$C_{net,m}^{t} = [\max(P_{load,m}^{t} - P_{pro,m}^{t}, 0) c_{m,s}^{t} + \min(P_{load,m}^{t} - P_{pro,m}^{t}, 0) c_{m,b}^{t}] \Delta t \tag{4}$$

$$C_{pun,m}^{t} = \max(P_{load,m}^{t} - P_{pro,m}^{t}, 0) c_{pun,m} \Delta t \tag{5}$$

To prevent the IESO from losing its status as a market player and a scenario where the SUT and DIESS directly trade energy with higher-level energy networks and thus disrupt the market with malicious bidding, the following constraints need to be imposed on the pricing strategy of the IESO:

$$\begin{cases} c_{n,b}^{t} < c_{buy,n}^{t} < c_{n,s}^{t} \\ c_{n,b}^{t} < c_{sell,n}^{t} < c_{n,s}^{t} \end{cases} \tag{6}$$

$$\sum_{t=1}^{T} c_{sell,n}^{t} \le T \cdot \overline{c}_{n,s,\max}^{t} \tag{7}$$

3.2. Distributed Integrated Energy Supply System Model

The DIESS optimizes the power generation of each active device in the system according to the energy price and carbon trading cost customized by the IESO, with the optimization objective of maximizing the revenue, which the following function can express:

$$\max F_{DIESS} = \sum_{m=1}^{M}\sum_{t=1}^{T}\left(C_{buy,m}^{t} - C_{DIESS,m}^{t}\right) - C_{co_2}^{DIESS} \tag{8}$$

The fuel cost includes both the MT and GB and the relationship between its fuel input cost and output power is expressed as a quadratic function according to its variable service efficiency characteristics:

$$C_{MGT,GB}^{t} = \alpha_{MGT}(P_{MT,e}^{t})^{2} + \beta_{MGT} P_{MGT,e}^{t} + \gamma_{MGT} + \alpha_{GB}(P_{GB,h}^{t})^{2} + \beta_{GB} P_{GB,h}^{t} + \gamma_{GB} \tag{9}$$

$$P_{MT,e}^{\min} \le P_{MT,e}^{t} \le P_{MT,e}^{\max} \tag{10}$$

$$P_{GB,h}^{\min} \le P_{GB,h}^{t} \le P_{GB,h}^{\max} \tag{11}$$

3.3. Energy Storage Equipment Model

The energy storage equipment can mitigate the power volatility of the system and maintain the power balance, which can be expressed as the following function:

$$\begin{cases} S_{soc,n}^{t} = S_{soc,n}^{t-1} + (\eta_{chr,n} P_{chr,n}^{t} - \frac{P_{dis,n}^{t}}{\eta_{dis,n}})\Delta t \\ S_{soc,n}^{\min} \le S_{soc,n}^{t} \le S_{soc,n}^{\max} \end{cases} \tag{12}$$

$$\begin{cases} \mu_{chr,n}^{t} P_{chr,n}^{\min} \le P_{chr,n}^{t} \le \mu_{chr,n}^{t} P_{chr,n}^{\max} \\ \mu_{dis,n}^{t} P_{dis,n}^{\min} \le P_{dis,n}^{t} \le \mu_{dis,n}^{t} P_{dis,n}^{\max} \end{cases} \tag{13}$$

3.4. Coupling Device Model

The rest of the system coupling equipment includes the HRSG, EB, P_2G, EC, and the AC. The energy hub (EH) is an input-output port model that describes the exchange and coupling relationship between energy, load, and network in a multi-energy system, involving the mutual transformation and distribution of multiple energy sources such as electricity, heat, and cold, with a high degree of flexibility. The generic model is:

$$L = CP \tag{14}$$

The energy conversion equipment inside the EH can realize the complementary co-existence between heterogeneous energy and can meet energy demand of various loads. Combined with the principle for the EH, energy conversion equipment inside the system can be uniformly expressed as the following function:

$$P_{i,n}^{t,out} = \eta_{i,n} P_{i,n}^{t,in} \tag{15}$$

$$\begin{cases} P_{i,n}^{\min,in} \le P_{i,n}^{t,in} \le P_{i,n}^{\max,in} \\ P_{i,n}^{\min,out} \le P_{i,n}^{t,out} \le P_{i,n}^{\max,out} \end{cases} \tag{16}$$

3.5. P_2G Equipment Carbon Reduction Model

P2G technology enables the synthesis of natural gas from electricity, which mainly includes two stages of electricity to make hydrogen and for hydrogen to produce methane. Its operation schematic is shown in Figure 3.

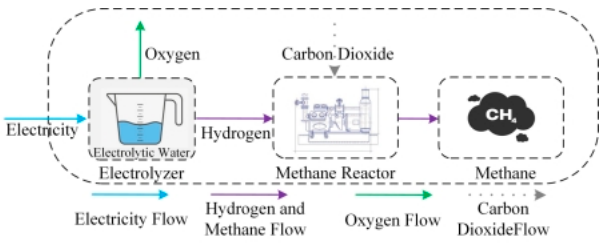


Figure 3. Schematic diagram of P_2G two-stage operation process.

In the first stage, the electrolyzer first electrolyzes water using the incoming electrical energy as a catalyst to produce hydrogen gas. In the second stage, hydrogen is chemically

reacted with carbon dioxide to produce methane. The relationship between its input electrical power and absorbed carbon footprint can be expressed follows:

$$P_{P_2G}^{t,in} = \frac{1}{3.6}\frac{LHV}{\eta_{P_2G}}V_{CH_4} \tag{17}$$

$$E_{A,P_2G} = \frac{V_{CH_4}}{V_{CH_4}^m}M_{CO_2}^m \tag{18}$$

3.6. Ladder-Type Carbon Trading Scheme

Compared to traditional carbon trading, the ladder-type carbon trading scheme has greater rewards and penalties for producers and better promotes low-carbon footprints. The following function can represent the carbon footprint allowance of the DIESS:

$$E_Q = E_{Q,MT} + E_{Q,GB} \tag{19}$$

Considering that the methane reactor in the electric-to-gas facility can absorb part of the CO_2 in the hydrogen-to-natural gas process, the actual carbon footprints are:

$$E_S = E_{T,MT} + E_{T,GB} - E_{A,P_2G} - E_Q \tag{20}$$

$$\begin{cases} E_{T,MT} = a_{MT} + b_{MT} \cdot P_{MT,e}^t + c_{MT} \cdot (P_{MT,e}^t)^2 \\ E_{T,GB} = a_{GB} + b_{GB} \cdot P_{GB,h}^t + c_{GB} \cdot (P_{GB,h}^t)^2 \end{cases} \tag{21}$$

The ladder-type carbon trading scheme is divided into multiple trading price tiers, and in correlation with the volume of purchased quotas, the higher the trading price in the corresponding interval. Therefore, the ladder-type carbon trading scheme cost of the DIESS is:

$$C_{co_2}^{DIESS} = \begin{cases} \lambda_{co_2} E_t^{DIESS} & E_t^{DIESS} \le l \\ \lambda_{co_2}(1+\alpha)(E_t^{DIESS} - l) + \lambda_{co_2} l & l \le E_t^{DIESS} \le 2l \\ \lambda_{co_2}(1+2\alpha)(E_t^{DIESS} - 2l) + \lambda_{co_2}(2+\alpha) l & 2l \le E_t^{DIESS} \le 3l \\ \lambda_{co_2}(1+3\alpha)(E_t^{DIESS} - 3l) + \lambda_{co_2}(3+3\alpha) l & 3l \le E_t^{DIESS} \le 4l \\ \lambda_{co_2}(1+4\alpha)(E_t^{DIESS} - 4l) + \lambda_{co_2}(4+6\alpha) l & 4l \le E_t^{DIESS} \end{cases} \tag{22}$$

3.7. Smart User Terminal Model

The SUT considers the utility of energy use by the user, combines the energy price information and IDR set by the IESO, and formulates a reasonable energy use plan by optimizing the scheduling of flexible loads to achieve the objective of maximizing consumer surplus, i.e., the difference between the utility function of the user and the cost of energy use can be expressed as the following function:

$$\max F_{SUT} = \sum_{n=1}^{N}\sum_{t=1}^{T}(U_{SUT,n}^t - C_{sell,n}^t) \tag{23}$$

In this paper, a quadratic utility function is used to characterize the energy use utility of users' energy use behavior, and its expression is:

$$U_{SUT,n}^t = \sum_{n=1}^{N}\sum_{t=1}^{T}[v_n P_{load,n}^t - \frac{u_n}{2}(P_{load,n}^t)^2] \tag{24}$$

3.8. Integrated Demand Response Model

IDR can be fully integrated with current research advances in communication technologies, distributed energy storage and distributed energy conversion devices to effectively stimulate load flexibility in the context of integrated energy networks. The IDR model can be expressed as the following function:

$$P_{load,n}^{t} = P_{load,n,0}^{t} + P_{tran,n}^{t} + P_{reduce,n}^{t} \tag{25}$$

$$\begin{cases} P_{tran,n}^{t,after} = P_{tran,n}^{t} + \Delta P_{tran,n}^{t} \\ \Delta P_{tran,n}^{t} = \mu_{tran,n}^{t,in} P_{tran,n}^{t,in} - \mu_{tran,n}^{t,out} P_{tran,n}^{t,out} \\ \sum_{t=1}^{T} \Delta P_{tran,n}^{t} = 0 \\ \mu_{tran,n}^{t,in} + \mu_{tran,n}^{t,out} = 1 \\ \tau_{tran,n}^{\min} \le \Delta P_{tran}^{i}(t) \le \tau_{tran,n}^{\max} \end{cases} \tag{26}$$

$$\begin{cases} P_{reduce,n}^{t,after} = P_{reduce,n}^{t} - \Delta P_{reduce,n}^{t} \\ \Delta P_{reduce,n}^{t} = \mu_{reduce,n}^{t} P_{reduce,n}^{t,reduce} \\ \tau_{reduce,n}^{\min} \le \Delta P_{reduce,n}^{t,reduce} \le \tau_{reduce,n}^{\max} \\ \sum_{t=1}^{T} \Delta P_{reduce,n}^{t} \le \lambda_{reduce,n} \end{cases} \tag{27}$$

4. Units Stackelberg Game Framework

4.1. Basic Concept

Upper layer: the IESO sets time-of-day energy prices based on energy flow information, to maximize self-interest.

Lower layer: (1) the DIESS optimizes the operational dispatch of individual components within the infrastructure according to the energy price and load demand at the energy-using end set by the upper layer to maximize its revenue. (2) the SUT rationalizes its energy use behavior to maximize consumer surplus according to energy price and supply situation.

In summary, the optimal operation of both the supply and the demand hinges on the pricing mechanism formulated by the IESO. Their optimization results will, in turn, react to the pricing strategy of the IESO, and this power transaction mechanism aligns with the principles of dynamic game theory. Therefore, this paper takes the IESO as the leader and the DIESS and SUT as the followers and establishes a single-leader multi-follower Stackelberg framework, which can be expressed as:

$$\begin{cases} G = \{N; \{IESO; DIESS; SUT\}\} \\ \delta_{IESO} = \left\{ c_{sell}^{n}; c_{buy}^{n} \right\} \\ \rho_{DIESS} = \left\{ P_{DIESS}^{e}; P_{DIESS}^{h} \right\} \\ \rho_{SUT} = \left\{ P_{SUT}^{e}; P_{SUT}^{h} \right\} \end{cases} \tag{28}$$

(1) Participants: the IESO, DIESS, and SUT form the three decision-makers within this strategic interaction, and the set of players is expressed as:

$$N; \{IESO; DIESS; SUT\} \tag{29}$$

(2) Strategies: The IESO strategy is responsible for setting prices for energy purchased and sold throughout the day, represented by the following vector:

$$\delta_{IESO} = \left\{ c_{sell}^{n}; c_{buy}^{n} \right\} \tag{30}$$

The Decision Scheme of the DIESS is the power output of each device in the system, which can be expressed as:

$$\rho_{DIESS} = \left\{ P_{DIESS}^{e}; P_{DIESS}^{h} \right\} \tag{31}$$

The Decision Scheme of the SUT is the power optimization case for flexible loads, which can be expressed as:

$$\rho_{SUT} = \left\{ P_{SUT}^{e}; P_{SUT}^{h} \right\} \tag{32}$$

(3) Earnings: The benefits for each participant are the objective functions defined by Equations (1), (8) and (23), respectively.

4.2. Analysis of Equilibrium Existence and Mathematical Rigor

The proposed bi-level optimization model essentially describes a dynamic interaction among the IESO, DIESS, and SUT, which must be mathematically scrutinized to ensure the validity of the subsequent numerical simulations. To establish this theoretical foundation, we define the interactive decision-making process as a single-leader–multi-follower game, which can be expressed as:

$$A = \{(IESO) \cup (DIESS, SUT); \Psi_L, \Psi_F; F_L, F_F\} \tag{33}$$

Here, the existence of an equilibrium point is the primary concern, as it guarantees that a stable operating point can be reached where no player has an incentive to unilaterally deviate from their strategy.

According to the Fan-Glicksberg fixed-point theorem, a Stackelberg equilibrium is inherently guaranteed if the strategy spaces are non-empty, compact, and convex, and the objective functions remain continuous over these domains. In our framework, the followers' feasible region Ψ_F is strictly governed by the physical coupling constraints and energy balance requirements detailed in Section 3. Since variables such as the power output of the MT and the conversion rates of P_2G are confined within finite capacity bounds, the strategy space can be formally represented as a closed and bounded subset of Euclidean space:

$$\Psi_F = \left\{ P \in R^n \mid AP \leq b, P^{min} \leq P \leq P^{max} \right\} \tag{34}$$

This formulation satisfies the topological requirement of compactness. It is also important to address the continuity of the objective functions, particularly given the inclusion of the ladder-type carbon trading mechanism. Although Equation (22) introduces a piecewise linear structure, the cost function remains globally continuous because the cost limits at each emission threshold l_k are mathematically consistent from both directions:

$$\lim_{E \to l_k^-} C_{carb}(E) = \lim_{E \to l_k^+} C_{carb}(E) \tag{35}$$

This mathematical continuity, paired with the compact strategy spaces, ensures that the game possesses at least one stable equilibrium solution. However, we must candidly acknowledge that proving the absolute uniqueness of such an equilibrium is a significantly more complex task. In an integrated energy system, the leader's objective function is

coupled with the followers' responses, creating a bilinear structure. The underlying curvature of this optimization landscape is determined by the Hessian matrix of the leader's profit function:

$$\nabla^2 F_L = 2\nabla B^*(\lambda) + \lambda \nabla^2 B^*(\lambda) \tag{36}$$

Because the followers' response mapping $B^*(\lambda)$ is often an implicit and non-linear function of the pricing signal, the Hessian matrix $\nabla^2 F_L$ tends to be indefinite across various regions of the strategy space. This implies that the solution landscape is likely multi-modal rather than strictly convex, which directly justifies our use of a heuristic approach for the outer-layer problem. Furthermore, the ladder-type carbon price signal exhibits non-smoothness at the transition boundaries, where the marginal cost changes abruptly:

$$\left.\frac{dC_{carb}}{dE}\right|_{l_k^-} < \left.\frac{dC_{carb}}{dE}\right|_{l_k^+} \tag{37}$$

These "kinks" in the response surface render traditional gradient-based analytical methods or KKT-reformulation techniques largely inapplicable, as they are prone to being trapped in local optima or failing due to non-differentiability. Consequently, the GA–CPLEX hybrid framework is employed as a strategic necessity. Utilizing the genetic algorithm to explore the non-convex pricing space and the CPLEX solver to ensure the deterministic optimality of the followers' best response is shown below:

$$\min F_F(\lambda^*, \mathbf{P}) \quad \text{s.t.} \quad \mathbf{P} \in \Psi_F \tag{38}$$

This nested logical loop ensures that each iteration is grounded in a rigorous optimal response, ultimately leading to a robust approximation of the Stackelberg equilibrium that respects both the physical limits and the economic incentives of the distributed energy subjects.

4.3. Solution Methodology: The Strategic GA–CPLEX Framework

To address the challenges posed by the non-smooth ladder-type carbon pricing and the non-convex bilinear coupling intrinsic to our bi-level model, we developed a hybrid GA–CPLEX solution framework grounded in the philosophy of functional decoupling. This architecture strategically partitions the optimization into two distinct layers: the outer layer genetic algorithm (GA) acts as a global "explorer," leveraging its gradient-free nature to navigate the non-differentiable pricing space and "hop" over the numerical pitfalls created by policy thresholds; meanwhile, the inner-layer CPLEX solver serves as a deterministic "executor." Once the pricing strategy is fixed by the outer layer, the followers' response problem reduces to a standard mixed-integer linear programming task, which CPLEX resolves with absolute mathematical rigor via the branch-and-cut algorithm.

The operational logic follows a nested "Search-and-Solve" loop. Initially, a population of pricing candidates is generated within the feasible domain. Each candidate is then transmitted to the inner layer, where CPLEX efficiently identifies the optimal energy responses for the DIESS and SUT. Based on these responses, the IESO's total profit is mapped as a fitness score, which subsequently drives the evolutionary operators—selection, crossover, and mutation—to refine the pricing strategies. To provide a formal assessment of the solver's efficiency, we define its computational complexity as follows:

$$C_{total} = O(G_{max} \cdot N_{pop} \cdot T_{MILP}) \tag{39}$$

In this context, the "search breadth" is determined by the maximum generation and the population size, while the "computational depth" is dictated by the solving time of a single

MILP iteration. Given that the integer variables remain manageable at the community scale, this decoupled structure effectively shields the process from the exponential "state explosion" often encountered in monolithic bi-level solvers. Its spatial complexity remains linear with respect to the decision variables, ensuring a lightweight memory footprint.

To ensure transparency and reproducibility, the framework is configured with hyper-parameters determined through preliminary sensitivity analyses, as summarized in Table 2. This synergy between heuristic exploration and deterministic precision not only provides the resilience needed to handle non-smooth policy constraints but also establishes a stable foundation for potential deployment on industrial-grade controllers.

Table 2. Key Parameter Configurations for the GA–CPLEX Framework.

Parameter	Value
Population Size (N_{pop})	50
Max Generations (G_{max})	200
Crossover/Mutation Rate	0.8/0.05
Stopping Criteria	$\Delta f < 10^{-4}$

5. Analysis of Example

5.1. Simulation Data

To validate the proposed IES distributed collaborative optimization operation scheme, a community-scale IES containing multi-energy coupling and conversion devices is utilized as a case study. The system framework incorporates an IESO as the coordinator, with its physical structure comprising WTs, PV arrays, MTs, P_2G units, and multi-form energy storage devices. As illustrated in Figure 4, the system operation is characterized by its input–output energy balance: the input side primarily consists of volatile renewable energy generated from WTs and PV, while the output side must satisfy the heterogeneous demands for electricity, heat, and cold loads from the SUT. This configuration provides a complex, multi-agent environment to test the interactive game strategies and the effectiveness of the collaborative optimization model.

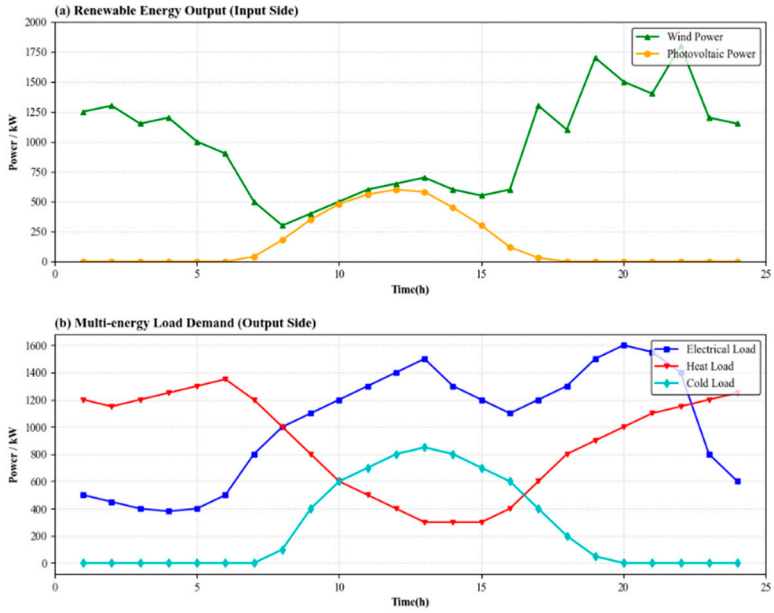


Figure 4. Typical daily curves of input renewable energy and output load demands.

On the input side, renewable energy generation primarily consists of the PV and WT, which serve as the foundational energy supply for the system. On the output side, the system must satisfy heterogeneous load requirements. Specifically, the electrical load exhibits dual peaks at 12:00 and between 18:00 and 22:00, reaching a maximum amplitude of approximately 1500 kW. The heat demand peaks during the early morning hours with a maximum amplitude near 1200 kW, while the cold demand reaches its highest point of approximately 800 kW between 9:00 and 15:00.

The significant temporal mismatch and amplitude variations between the input energy and output loads necessitate an effective pricing mechanism. Under baseline conditions, the peak hour electricity tariff is set at 0.173 $/kWh, the valley tariff at 0.058 $/kWh, and the usual tariff at 0.12 $/kWh. Additionally, the heat tariff is constrained between an upper limit of 0.072 $/kWh and a lower limit of 0.021 $/kWh. The example is solved using a genetic algorithm nested with a CPLEX solver, and the example scenario is shown below.

Scenario 1: Consider the IDR without carbon trading mechanisms.

Scenario 2: Consider the IDR and traditional carbon trading mechanisms, introducing P_2G equipment and quantifying their carbon reduction capacity.

Scenario 3: Consider the IDR and ladder-type carbon trading scheme, introducing P_2G equipment and quantifying their carbon reduction capacity.

5.2. Discussion of the Findings of the Stackelberg Game Optimization Strategy

For scenario 1, the iterative optimization process of the DIESS, IESO, and SUT is shown in Figure 5. It can be seen that the convergence trends of the leader and the follower are different. With the increase in the number of game iterations, the gain of the IESO is increasing, while the gain of the DIESS and the consumer surplus of the SUT are decreasing, which reflects the dynamic game process among the three players. When the Stackelberg equilibrium is reached, the operating strategy does not change, meaning no participant can independently change its own operating strategy and thus gain more revenue. Finally, the returns of the IESO and DIESS are stabilized at $8621.77 and $12,395.47, respectively, and the consumer surplus of the SUT is stabilized at $14,381.32.

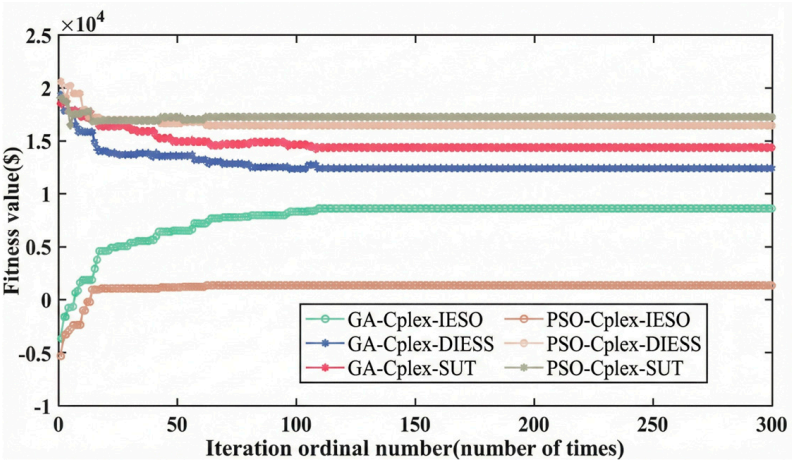


Figure 5. Comparison of game equilibrium convergence results.

To provide a rigorous justification for the proposed GA–CPLEX framework, we conducted a comprehensive performance comparison with several established bi-level optimization solvers: KKT-based exact reformulation, ADMM-based decentralized coordination, and the standard PSO–CPLEX heuristic. While PSO–CPLEX is a widely recognized benchmark in energy system studies due to its simplicity and balanced search–exploitation capability, our investigation reveals its limitations when faced with the non-smooth "kinks"

of ladder-type carbon signals. To eliminate the influence of random initialization on the algorithm's performance and to provide a rigorous evaluation of robustness, each candidate methodology was executed for 50 independent simulation runs under identical hardware configurations. This statistical approach allows for a comprehensive assessment of not only the optimal solution but also the stability and reliability of the solvers in a complex, non-smooth search space.

According to data in Table 3, the GA–CPLEX framework demonstrates a superior balance between solution quality and computational robustness. Specifically, while the KKT-based approach is theoretically faster, it suffered from severe numerical instability in our tests. The piecewise nature of the ladder-type carbon trading creates non-differentiable boundaries where the Big-M linearization required for KKT conditions often fails to find a feasible descent direction, leading to a low success rate of only 32%.

Table 3. Quantitative performance comparison of different solution methodologies.

Methodology	Avg. Total Cost ($)	Comp. Time (s)	Iterations to Converge	Success Rate (%)
GA–CPLEX	43,050.2	145.6	82	99%
PSO–CPLEX	44,720.5	112.4	126	94%
KKT-based	48,150.8	42.5	\	32%
ADMM	45,980.3	288.7	450	68%

Similarly, although the ADMM is highly regarded for its decentralized nature, it exhibited persistent oscillations in our bi-level game environment. The strong non-convex coupling between the IESO's pricing and the DIESS's response power prevents the dual variables from converging smoothly, resulting in high computational burden without achieving lower cost.

Interestingly, our proposed framework not only yielded the lowest average cost but also maintained an exceptionally low standard deviation across all successful runs. This indicates that by offloading the followers' complex physical constraints to a deterministic CPLEX engine and allowing the outer-layer GA to explore the non-smooth pricing space, we effectively "shield" the optimization process from the pitfalls of local optima and gradient failures. These results confirm that GA–CPLEX is not merely a choice of convenience, but a strategically necessary tool for managing the intricate trade-offs in low-carbon integrated energy systems.

Figure 6 presents the pricing strategy of the leader IESO for Scenarios 2 and 3. In Figure 6a, the broken lines in black and dark blue denote the time-varying pricing and grid injection schemes from the upper-level grid, respectively. Constrained by Equation (6), the IESO establishes rates within this range to offer the DIESS and SUT more favorable price signals than the external grid, thereby boosting the revenue for all parties.

The tariff rate set by the IESO is basically in line with the trend of time-sharing tariff but never exceeds cost of power acquired directly from the upstream network by the SUT, which saves SUT's electricity purchase cost; the electricity purchase price set by the IESO is basically in line with the fluctuation trend of electricity load curve, which can stimulate the DIESS to increase electricity generation during the peak load period to enhance its electricity sales revenue; at the same time, due to the increase in electricity sales by the DIESS, the IESO's electricity purchase from the superior grid decreases under the condition of a certain electricity load, and the electricity purchase cost also decreases; a win-win situation between the leader and the follower is realized. The thermal pricing structure analysis in Figure 6b is analogous to electricity tariffs and will not be duplicated here.

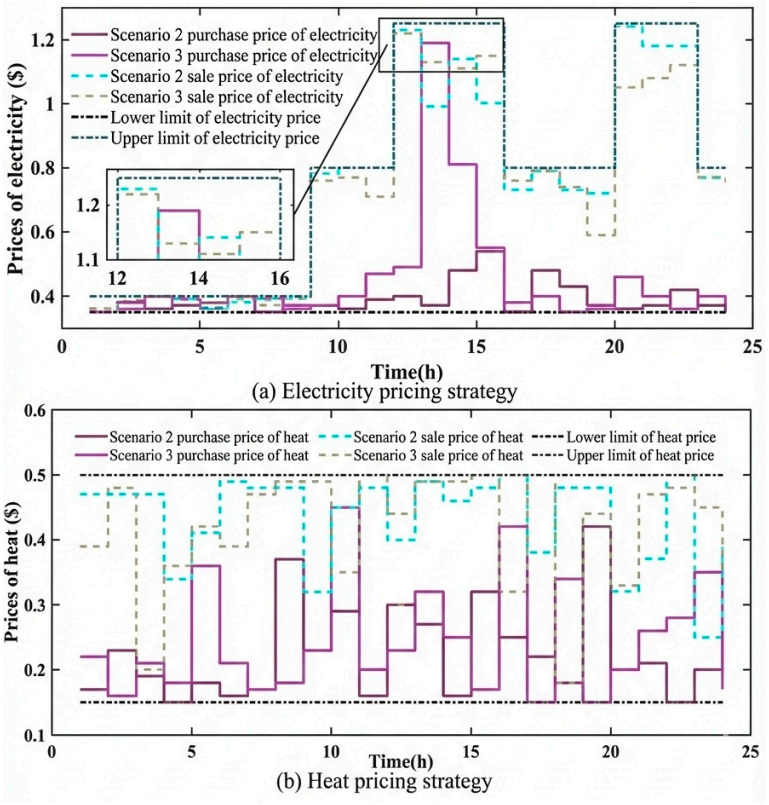
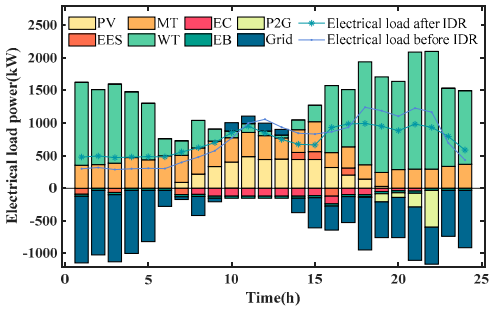


Figure 6. Pricing strategy for IESO in Scenario 2 and Scenario 3.

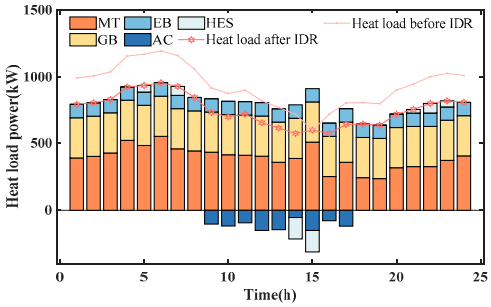
In addition, considering the IDR based on developing an energy pricing strategy can fully stimulate load flexibility on the customer side. Figure 7 shows the optimal scheduling of electrical, heat, and cold load for the two scenarios. From Figure 7a,b, It is evident that under stimulation of electricity price, 11:00–13:00 and 20:00–22:00 are the double peak hours of electricity load and purchase price, and after customer-side optimization, the peak load drops significantly and shifts to the double low hours of electricity load and purchase price, 0:00–8:00 and 23:00–24:00, to realize the "shaving peaks and filling troughs" of the power demand profile. In addition, the cold energy in this paper adopts the same price strategy as the heat energy. From Figure 7c–f, it can be seen that both heat and cold loads are reduced overall, and it is worth noting that the heat load is at a low point from 13:00 to 16:00, and the heat load is reduced less to ensure the energy comfort of the users. After optimization, the energy purchase cost of the SUT is reduced, and the consumer surplus and utility function are increased, as shown in Table 4.

Table 4. Energy use indicators of the SUT before and after IDR are considered in scenarios 2 and 3.

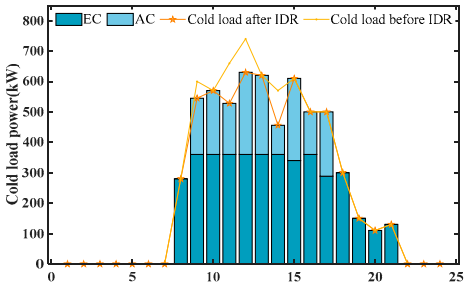
	Scenario	Utility Function ($)	Energy Purchase Cost ($)	Consumer Surplus ($)
Before IDR	Scenario 2	37,206	27,236	9970
	Scenario 3	37,206	26,726	10,480
After IDR	Scenario 2	38,085	24,323	13,762
	Scenario 3	38,011	23,505	14,506



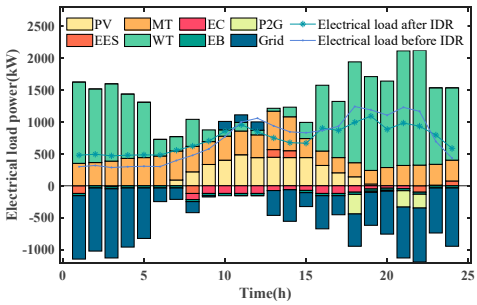
(**a**) Electrical load scheduling outcomes for scenario 2



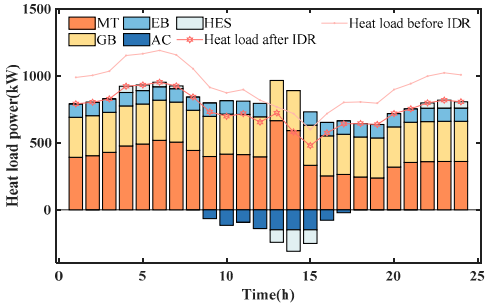
(**b**) Heat load scheduling outcomes for scenario 2



(**c**) Cold load scheduling outcomes for scenario 2

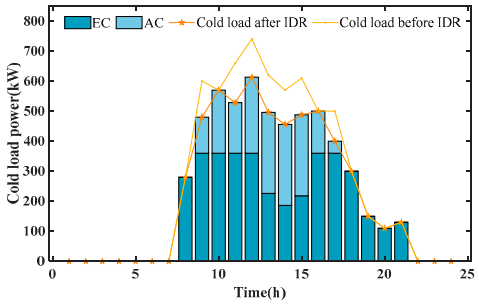


(**d**) Electrical load scheduling outcomes for scenario 3



(**e**) Heat load scheduling outcomes for scenario 3

Figure 7. *Cont.*



(**f**) Cold load scheduling outcomes for scenario 3

Figure 7. Electrical, heat and cold load scheduling outcomes for scenarios 2 and 3.

5.3. Benefit Analysis Under Different Pricing Strategies

Tables 5–7 show the scheduling results under Scenario 2 and Scenario 3. As indicated in Tables 5–7, the aggregate profits and carbon footprint of the DIESS under Scenario 3, which considers the ladder-type carbon trading scheme, differ from our previous inertial perception of the ladder-type carbon trading scheme in that both its carbon footprint and total benefits increase. There are two reasons for this. The first reason is the setting of the ladder-type carbon trading scheme parameters in Scenario 3, which will be analyzed in subsequent sections of this paper; the second reason is that due to the existence of the gaming alliance, the optimization goal of the DIESS is no longer simply itself, but the optimal scheduling strategy under the influence of the alliance composed of the DIESS, IESO and SUT as a whole, so the scheduling strategy of the DIESS should be analyzed in conjunction with the decisions of the IESO and SUT.

Table 5. Benefit analysis of IESO under different pricing strategies.

Scenario	Energy Sales Revenue ($)	Energy Purchase Cost ($)	Energy Interaction Gains ($)	Penalty Cost ($)	Revenue ($)
Scenario 2	28,454.85	16,951.07	4132.36	459.76	11,044.02
Scenario 3	27,787.63	18,923.85	4282.65	386.44	8477.34

Table 6. Benefit analysis of DIESS under different pricing strategies.

Scenario	Energy Sales Revenue ($)	Energy Supply Cost ($)	Carbon Footprints (kg)	P_2G Carbon Footprint Reductions (kg)	Total Revenue ($)
Scenario 2	16,780.00	5396.49	26,851.16	128.17	10,525.83
Scenario 3	18,768.55	5489.27	27,887.24	106.44	12,073.09

Table 7. Benefit analysis of SUT under different pricing strategies.

Scenario	Effectiveness Function ($)	Energy Purchase Cost ($)	Consumer Surplus ($)	Total IDR Percentage (%)	Total Affiliate Revenue ($)
Scenario 2	38,084.88	24,322.50	13,762.37	10.12	35,332.22
Scenario 3	38,010.96	23,505.03	14,505.93	10.32	35,056.36

Combined with Figure 6, we can see that the pricing strategy of the IESO in Scenario 3 is more beneficial to DIESS profitability than Scenario 2, which is mainly reflected in the fact that the energy purchase price set in Scenario 3 is generally larger than that in Scenario 2, especially during the peak electric load hours; the difference in the purchase price is noticeable. Figure 8 shows the amount of energy sold and the revenue from energy sales of

the DIESS in the two scenarios mentioned above. Taking the 13th and 21st points in the figure as examples, the 13th point indicates that the amount of electricity sold by the DIESS in Scenario 3 is greater than that of the IESO, and since the price of electricity purchase is also at its peak at this time, the DIESS can gain more revenue than Scenario 2 by selling electricity at that moment; the 21st point indicates that the amount of electricity sold in Scenario 3 is lower than that of Scenario 2, but due to the difference in the power purchase price set in the two scenarios, Scenario 3, in turn, can get more sales energy gains. Therefore, the energy supply gain of the DIESS in Scenario 3 is higher than in Scenario 2.

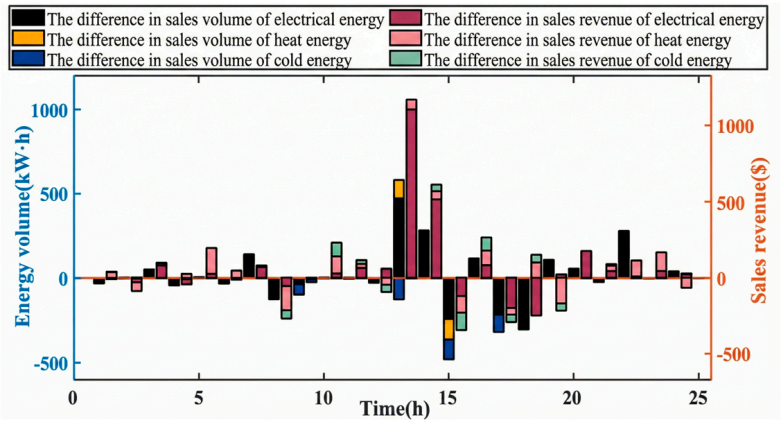


Figure 8. Distribution of the difference between energy sales volume and energy sales revenue for Scenario 3 and Scenario 2.

If the pricing strategies for Scenario 2 and Scenario 3 are swapped, the optimization results of the DIESS, IESO and SUT are shown in Table 8. For Scenario 2, when it adopts the pricing strategy of Scenario 3, the carbon emissions decrease from 27,595.24 kg to 26,851.16 kg, the total benefits of the DIESS increase slightly, and the total benefits of the IESO, consumer surplus and the total benefits of the gaming coalition all decrease; For Scenario 3, when it uses the pricing strategy of Scenario 2, there is no significant change in the carbon emissions and total benefits of the DIESS. Still, there is a significant decrease in both consumer surplus and total benefits of the gaming alliance. It confirms the above—when the game reaches convergence, no party can gain more by changing its strategy.

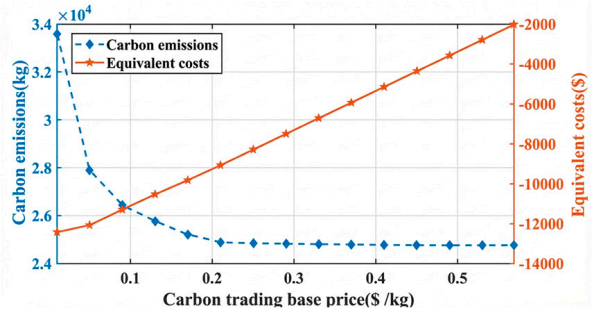
Table 8. Benefit analysis of pricing strategy swap for scenario 2 and scenario 3.

	Scenario	Equivalent Output of MT (kW·h)	Equivalent Output of GB (kW·h)	Carbon Footprints (kg)	Total Amount of Energy Sold by DIESS (kW·h)	Total Revenue of DIESS ($)	Total Revenue of IESO ($)	Consumer Surplus of SUT ($)	Total Affiliate Revenue ($)
Pricing strategy for scenario 2	Scenario 2	17,988.29	7200.00	27,595.24	52,842.68	10,525.83	11,044.03	13,762	35,331.86
	Scenario 3	18,349.90	7200.00	26,851.16	53,118.38	12,016.64	8958.05	13,580	34,554.69
Pricing strategy for scenario 3	Scenario 2	19,296.72	7152.33	30,044.41	53,830.01	12,483.03	8477.40	13,343	34,303.43
	Scenario 3	18,297.57	7200.00	27,887.24	52,910.42	12,073.09	8833.74	14,505.93	35,412.76

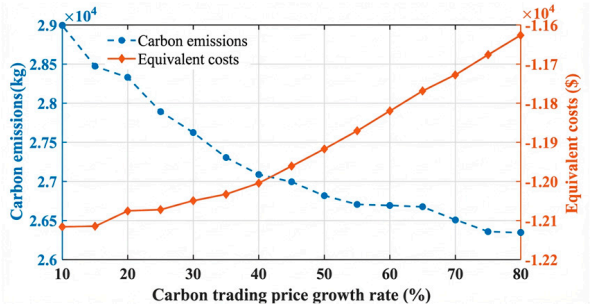
5.4. Analysis of Benefits Under Different Ladder-Type Carbon Trading Scheme Parameters

The internal operational strategy of the DIESS is highly sensitive to the specific settings of the tiered carbon trading framework. However, prevailing research predominantly concentrates on the variations in baseline pricing, with scant attention paid to the influence of the interval width and the price escalation factor on the system's performance. Conse-

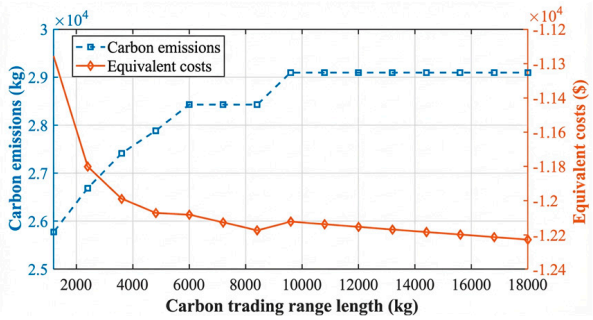
quently, this paper analyzes the effects of the above; the aforementioned trio of variables on the carbon footprint and overall operational outlays of the DIESS, are depicted in Figure 9.



(**a**) Benefit assessment of emission exchange baseline price



(**b**) Benefit assessment of emission exchange price growth rate



(**c**) Benefit assessment of emission exchange range length

Figure 9. Benefit assessment of different emission exchange mechanism parameters.

As shown in Figure 9a, when the base price of carbon trading is below 0.21 $/kg, the tiered carbon trading scheme imposes more stringent limitations on emission levels as the price increases. Consequently, the system adopts emission mitigation strategies to minimize total costs, resulting in a progressive decline in the carbon footprint. However, once the base price exceeds 0.21 $/kg, the carbon footprint tends to stabilize. This is because the output of carbon dioxide-generating equipment has already been compressed to its minimum level, leaving no further room for the system to reduce emissions. However, the equivalent cost continues to rise.

As illustrated in Figure 9b, an escalation in the price growth factor drives up carbon trading expenses. To mitigate these costs, the system optimizes the dispatch of internal units to lower the carbon footprint. Notably, within the price growth interval of [75%, 80%], the equipment output distribution achieves equilibrium to satisfy thermal demand, causing the variation in carbon emissions to plateau.

From Figure 9c, it can be seen that when the length of the carbon trading interval is at (1200 kg, 9800 kg], the number of steps of the emission exchange mechanism gradually decreases as length for the emission exchange interval increases, so equivalent cost gradually decreases, but the carbon footprint gradually increases; in the range of (14,600 kg,

18,200 kg), the increase in the length of the interval will not lead to the change in the number of steps, so the increase in carbon footprints and the decrease in equivalent cost are both slow; when the interval length is large enough, there will be a scenario in which the emission exchange mechanism only works on the first step number and the carbon trading baseline price. Then enlarging the step increment exerts no influence on the carbon footprints and the equivalent cost of the system.

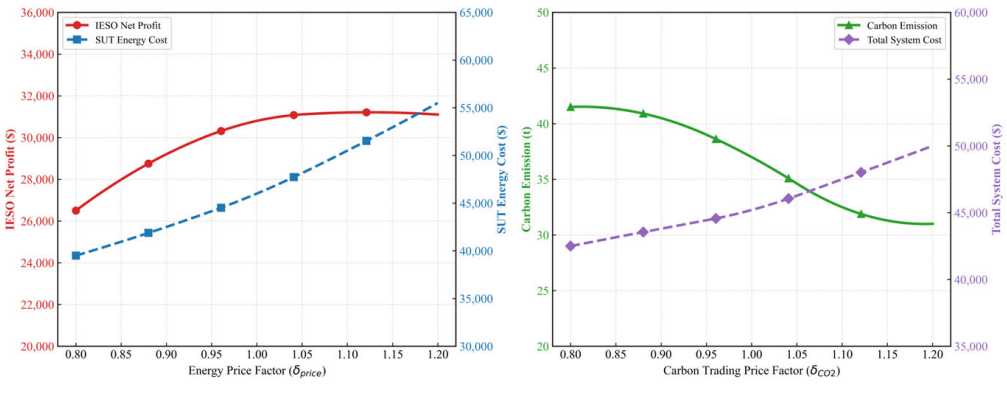
A deeper examination of the simulation results reveals that the integration of the ladder-type carbon trading mechanism fundamentally alters the strategic interaction between the IESO and prosumers. Unlike traditional models where carbon costs are treated as fixed overhead, the proposed game-theoretic framework uncovers a non-linear cost-transmission law. Specifically, as the system enters a higher carbon price interval, the IESO strategically adjusts its pricing leverage not merely to maximize immediate revenue, but to actively induce a 'behavioral shift' in the DIESS and SUT.

This phenomenon is evidenced by the increased operational elasticity of P_2G during peak emission periods. By acting as an operational buffer, P_2G allows prosumers to mitigate high-step carbon penalties through green hydrogen conversion, effectively decoupling localized energy demand from systemic emission intensity. Furthermore, the convergence process in Figure 6 substantiates that the Stackelberg equilibrium reached in Scenario 3 represents a superior 'Carbon-Economic' Pareto balance. The IESO accepts a marginal reduction in pricing flexibility in exchange for a significantly more resilient and low-carbon operation of the distribution network; a result that underscores the synergistic value of multi-agent coordination under tiered policy constraints.

5.5. Robustness and Sensitivity Analysis Under Fluctuating Environments

To verify the stability of the proposed Stackelberg game strategy and the regulatory adaptability of the ladder-type carbon trading mechanism, we conducted a comprehensive sensitivity analysis regarding key pricing parameters and environmental uncertainties.

To evaluate the market pricing mechanism, the energy price factor δ_{price} was varied from 0.8 to 1.2. As illustrated in Figure 10a, the net profit of the IESO follows a logical saturation trajectory rather than increasing linearly. In the initial phase where δ_{price} is below 1.0, raising prices directly boosts profit margins. However, once the price factor exceeds the equilibrium point, profit growth stagnates and the curve begins to flatten. This phenomenon is driven by the Integrated Demand Response mechanism on the user side. Faced with excessive prices, the user side proactively reduces electrical and thermal loads or shifts consumption to avoid high costs. This rational resistance from users offsets the benefits of higher unit prices, effectively preventing the IESO from monopolistic overpricing and confirming that the algorithm has successfully located a robust global optimal point.



(a) Sensitivity to Energy Price Factor (b) Sensitivity to Carbon Price Factor

Figure 10. Sensitivity of System Performance to Uncertainties.

Complementing this economic analysis, the decarbonization sensitivity was examined under varying carbon trading price factors δ_{CO2}, as shown in Figure 10b. The carbon emission curve exhibits a smooth inverse S-shape characteristic, reflecting the physical realities of the system. In the low carbon price zone where δ_{CO2} is less than 0.9, the system lacks the financial incentive to operate high-cost P_2G and CCS equipment, resulting in a slow reduction rate. As the carbon price rises to the range between 0.9 and 1.1, the ladder-type mechanism triggers higher penalty tiers, compelling the system to rapidly ramp up low-carbon technologies and leading to a significant decline in emissions. Finally, at extremely high carbon prices where δ_{CO2} exceeds 1.1, the reduction rate slows down again. This behavior indicates a technical bottleneck, as the system approaches its physical capacity limit for emission reduction. Although the total system cost increases by 10.5% in the high-carbon-price scenario, emissions are reduced by 21.5%, proving that the mechanism effectively forces a trade-off between economic cost and environmental benefit.

Beyond parametric sensitivity, the operational resilience of the proposed method was tested against supply-side uncertainty. In a worst-case scenario where renewable energy output fluctuates by -20%, the system compensates for the energy deficit by increasing gas turbine output and grid imports. While this inevitably raises the total operating cost by 11.2% due to the high marginal cost of backup energy, the system maintains stable operation without convergence failure. The P_2G units and thermal storage tanks act as effective energy buffers to absorb stochastic shocks, demonstrating that the multi-agent interaction mechanism maintains operational resilience even under severe supply-side fluctuations.

6. Conclusions

This paper establishes a Stackelberg game model for a distributed integrated energy system, featuring the IESO as the leader and the DIESS and SUT as followers. The energy flow and pricing are used as decision variables to optimize the benefits of all participants. The main findings and scientific originalities are summarized as follows:

(1) The dynamic transmission law of carbon costs in a multi-agent game is revealed. This research moves beyond traditional centralized models to demonstrate how the ladder-type carbon trading scheme transmits cost signals from the IESO's pricing leverage to both the supply and demand sides in real time. This mechanism induces game subjects to change their original operating inertia, providing a new perspective on the role of carbon markets in a multi-energy coupling environment.

(2) A low-carbon coupling dispatch strategy based on refined P2G modeling is formulated. By introducing a two-stage P2G process integrated with ladder-type carbon trading, this work identifies P2G as a strategic "buffer" that regulates the pricing elasticity of the entire system. This refined approach uncovers the non-linear relationship between conversion efficiency and economic returns, achieving a 10.7% improvement in total cost efficiency compared to traditional fixed-price mechanisms.

(3) A hybrid GA-CPLEX optimization framework is designed and validated to balance computational efficiency and solution quality. By strategically partitioning the global pricing search from deterministic linear programming, the framework effectively avoids local optima and handles the non-smooth "kinks" of carbon signals with a 99% success rate. Sensitivity analysis confirms the model's resilience, maintaining stable equilibrium points.

In conclusion, the proposed method effectively stimulates load flexibility through IDR and optimizes the interest distribution among the IESO, DIESS, and SUT. While this paper considers a single DIESS model, future research will explore the coordination of clustered DIESS units within complex energy market environments.

https://doi.org/10.3390/electronics15040721

Author Contributions: Conceptualization, W.T.; methodology, W.T. and J.L.; validation, J.L.; formal analysis, P.S.; supervision, M.Y. All authors have read and agreed to the published version of the manuscript.

Funding: This research was funded by State Grid Corporation of China Science and Technology Project (SGJLSY00KJJS2501515), 'Research on Guiding Strategies for Multi-Grid Operator Tariff Formulation Considering User Electricity Characteristics in Songyuan Power Supply Company by 2025'.

Data Availability Statement: The original contributions presented in the study are included in the article, further inquiries can be directed to the corresponding author.

Conflicts of Interest: Author Weining Tang is employed by the company State Grid Jilin Electric Power Co., Ltd., Songyuan Power Supply Company and is currently a doctoral student at Northeast Electric Power University. The remaining authors declare that the research was conducted in the absence of any commercial or financial relationships that could be construed as a potential conflict of interest.

Abbreviations

The following abbreviations are used in this manuscript:

IES	Integrated energy system
DIESS	Directory of open access journals
IESO	Integrated energy system operator
SUT	Smart user terminal
IDR	Integrated Demand Response
P_2G	Power-to-Gas
MT	Micro Turbine
HRSG	Heat Recovery Steam Generator
GB	Gas Fired Boiler
EB	Electric Boiler
EC	Electric Chiller
AC	Absorption Chiller
WT	Wind Turbine
PV	Photovoltaic
EES	Electric Energy Storage
HES	Heat Energy Storage
EH	Energy Hub
LHV	Lower Heating Value
SOC	State of Charge
GA	Genetic Algorithm
PSO	Particle Swarm Optimization
ADMM	Alternating Direction Method of Multipliers
KKT	Karush-Kuhn-Tucker

Nomenclature

Indices and sets

Symbol	Definition
i	Index for coupling devices
m, M	Index and total number of energy types
n, N	Index and total number of energy forms
t, T	Index and total number of time periods in scheduling cycle

Parameters

Symbol	Definition
$\bar{c}^t_{n,s,max}$	Upper limit of average selling energy price

$c^t_{buy,m}$	Price of IESO purchasing energy m from DIESS at time t
$c^t_{m,b}$	Price of IESO purchasing energy m from upper-level energy network at time t
$c^t_{m,s}$	Price of IESO selling energy m to upper-level energy network at time t
$c_{pun,m}$	Unit penalty cost for energy m
$c^t_{sell,m}$	Price of IESO selling energy m to SUT at time t
Δt	Time interval
$\alpha_{GB}, \beta_{GB}, \gamma_{GB}$	Fuel cost coefficients of GB
$\alpha_{MT}, \beta_{MT}, \gamma_{MT}$	Fuel cost coefficients of MT
$\eta_{i,n}$	Energy conversion efficiency of coupling device i for energy n
$P^{max}_{GB,h}, P^{min}_{GB,h}$	Upper and lower limits of GB thermal power
$P^{max,in}_{i,n}, P^{min,in}_{i,n}$	Upper and lower limits of input power for coupling device i
$P^{max,out}_{i,n}, P^{min,out}_{i,n}$	Upper and lower limits of output power for coupling device i
$P^{max}_{MT,e}, P^{min}_{MT,e}$	Upper and lower limits of MT electrical power
$\eta_{chr,n}, \eta_{dis,n}$	Charging and discharging efficiency of energy storage device n
$P^{max}_{chr,n}, P^{min}_{chr,n}$	Upper and lower limits of charging power for energy storage device n
$P^{max}_{dis,n}, P^{min}_{dis,n}$	Upper and lower limits of discharging power for energy storage device n
$S^{max}_{SOC,n}, S^{min}_{SOC,n}$	Upper and lower limits of capacity for energy storage device n
η_{P_2G}	Conversion efficiency of P2G equipment
LHV	Lower heating value of gas source
$M^m_{CO_2}$	Molar mass of CO_2
V_{CH_4}	Output volume of methane
$V^m_{CH_4}$	Molar volume of methane
a_{GB}, b_{GB}, c_{GB}	Carbon emission coefficients of GB
a_{MT}, b_{MT}, c_{MT}	Carbon emission coefficients of MT
α	Price growth rate of ladder-type carbon trading
$E_{Q,MT}, E_{Q,GB}$	Carbon emission quotas of MT and GB
l	Interval length of ladder-type carbon trading
λ_{co_2}	Benchmark price of ladder-type carbon trading
$P^t_{load,n,0}$	Baseline load of energy n at time t
$\rho_{reduce,n}$	Curtailable load ratio of energy n
$\rho_{tran,n}$	Transferable load ratio of energy n
v_n, u_n	User preference coefficients for energy n
$\xi_{reduce,n}$	Curtailment compensation coefficient of energy n

Variables

Symbol	Definition
$C^t_{buy,m}$	Energy purchasing cost of energy m at time t
$C^t_{net,m}$	Energy interaction cost of energy m at time t
$C^t_{pun,m}$	Penalty cost of energy m at time t
$C^t_{sell,m}$	Energy selling revenue of energy m at time t
F_{IESO}	Total revenue of IESO
$C^{DIESS}_{co_2}$	Carbon trading cost of DIESS
$C^t_{DIESS,m}$	Energy supply cost of energy m at time t
$C^t_{MT,GB}$	Fuel cost at time t
F_{DIESS}	Total revenue of DIESS
$P^t_{GB,h}$	Thermal power output of GB at time t
$P^{t,in}_{i,n}$	Input power of energy n for coupling device i at time t
$P^{t,out}_{i,n}$	Output power of energy n for coupling device i at time t
$P^t_{MT,e}$	Electrical power output of MT at time t
$\mu^t_{chr,n}$	Charging status indicator of energy storage device n at time t
$\mu^t_{dis,n}$	Discharging status indicator of energy storage device n at time t

$P^t_{chr,n}$	Charging power of energy storage device n at time t
$P^t_{dis,n}$	Discharging power of energy storage device n at time t
$S^t_{SOC,n}$	State of charge of energy storage device n at time t
E_{A,P_2G}	Carbon emissions absorbed by P2G equipment
E_Q	Total carbon emission quota
E_S	Carbon trading volume
$E_{T,MT}$, $E_{T,GB}$	Actual carbon emissions of MT and GB
F_{SUT}	Consumer surplus of SUT
$P^t_{load,n}$	Load demand of energy n at time t
$P^t_{pro,m}$	Purchasing power of energy m at time t
$P^t_{reduce,n}$	Curtailable load of energy n at time t
$P^t_{tran,n}$	Transferable load of energy n at time t
$U^t_{SUT,n}$	Utility function of energy n at time t

References

1. Yang, M.; Guo, Y.; Fan, F. Ultra-Short-Term Prediction of Wind Farm Cluster Power Based on Embedded Graph Structure Learning with Spatiotemporal Information Gain. *IEEE Trans. Sustain. Energy* **2025**, *16*, 308–322. [CrossRef]
2. Yang, M.; Jiang, Y.; Xu, C.; Wang, B.; Wang, Z.; Su, X. Day-ahead wind farm cluster power prediction based on trend categorization and spatial information integration model. *Appl. Energy* **2025**, *388*, 125580. [CrossRef]
3. Yang, M.; Shen, X.; Huang, D.; Su, X. Fluctuation Classification and Feature Factor Extraction to Forecast Very Short-Term Photovoltaic Output Powers. *CSEE J. Power Energy Syst.* **2025**, *11*, 661–670. [CrossRef]
4. Yang, M.; Wang, K.; Su, X.; Ma, M.; Wu, G.; Huang, D. Short-term photovoltaic output probability prediction method considering the spatio-temporal-condition dependence of prediction error. *CSEE J. Power Energy Syst.* 2023, *Early Access*. [CrossRef]
5. Dong, Z.; Zhao, J.; Wen, F.; Xue, Y. From Smart Grid to Energy Internet: Basic Concept and Research Framework. *Autom. Electr. Power Syst.* **2023**, *47*, 679–690.
6. Wang, C.; Lv, C.; Li, P.; Li, S.; Zhao, K. Multiple Time-scale Optimal Scheduling of Community Integrated Energy System Based on Model Predictive Control. *Proc. CSEE* **2019**, *39*, 6791–6803+7093.
7. Pan, H.; Gao, H.; Yang, Y.; Ma, W.; Zhao, Y.; Liu, J. Multi-type Retail Packages Design and Multi-level Market Power Purchase Strategy for Electricity Retailers Based on Master-slave Game. *Proc. CSEE* **2022**, *42*, 4785–4800.
8. Leng, R.; Li, Z.; Xu, Y. Two-stage Stochastic Programming for Coordinated Operation of Distributed Energy Resources in Unbalanced Active Distribution Networks with Diverse Correlated Uncertainties. *J. Mod. Power Syst. Clean Energy* **2023**, *11*, 120–131. [CrossRef]
9. Ju, L.; Tan, Z.; Li, H.; Tan, Q.; Yu, X.; Song, X. Multiobjective operation optimization and evaluation model for CCHP and renewable energy based hybrid energy system driven by distributed energy resources in China. *Energy* **2016**, *111*, 322–340. [CrossRef]
10. Yang, X.; Leng, Z.; Xu, S.; Yang, C.; Yang, L.; Liu, K.; Song, Y.; Zhang, L. Multi-objective optimal scheduling for CCHP microgrids considering peak-load reduction by augmented ε-constraint method. *Renew. Energy* **2021**, *172*, 408–423.
11. Zhou, X.; Ai, Q. Distributed economic and environmental dispatch in two kinds of CCHP microgrid clusters. *Int. J. Electr. Power Energy Syst.* **2019**, *112*, 109–126. [CrossRef]
12. Li, K.; Ye, N.; Li, S.; Wang, H.; Zhang, C. Distributed collaborative operation strategies in multi-agent integrated energy system considering integrated demand response based on game theory. *Energy* **2023**, *273*, 127137. [CrossRef]
13. Tan, J.; Li, Y.; Zhang, X.; Pan, W.; Ruan, W. Operation of a commercial district integrated energy system considering dynamic integrated demand response: A Stackelberg game approach. *Energy* **2023**, *274*, 126888. [CrossRef]
14. Li, S.; Zhang, L.; Nie, L.; Wang, J. Trading strategy and benefit optimization of load aggregators in integrated energy systems considering integrated demand response: A hierarchical Stackelberg game. *Energy* **2022**, *249*, 123678. [CrossRef]
15. Zhang, G.; Niu, Y.; Xie, T.; Zhang, K. Multi-level distributed demand response study for a multi-park integrated energy system. *Energy Rep.* **2023**, *9*, 2676–2689. [CrossRef]
16. Li, Y.; Wang, B.; Yang, Z.; Li, J.; Chen, C. Hierarchical stochastic scheduling of multi-community integrated energy systems in uncertain environments via Stackelberg game. *Appl. Energy* **2022**, *308*, 118392. [CrossRef]
17. Wu, Q.; Xie, Z.; Li, Q.; Ren, H.; Yang, Y. Economic optimization method of multi-stakeholder in a multi-microgrid system based on Stackelberg game theory. *Energy Rep.* **2022**, *8*, 344–351.
18. Liu, X.; Ji, Z.; Sun, W.; He, Q. Robust game-theoretic optimization for energy management in community-based energy system. *Electr. Power Syst. Res.* **2023**, *214*, 108939.

19. Hu, Y.; Zhang, M.; Wang, K.; Wang, D. Optimization of orderly charging strategy of electric vehicle based on improved alternating direction method of multipliers. *J. Energy Storage* **2022**, *55*, 105483. [CrossRef]
20. Zhang, N.; Yang, D.; Zhang, H.; Luo, Y. Distributed control strategy of DC microgrid based on consistency theory. *Energy Rep.* **2022**, *8*, 739–750. [CrossRef]
21. Cai, Y.; Lu, Z.; Pan, Y.; He, L.; Guo, X.; Zhang, J. Optimal scheduling of a hybrid AC/DC multi-energy microgrid considering uncertainties and Stackelberg game-based integrated demand response. *Int. J. Electr. Power Energy Syst.* **2022**, *142*, 108341.
22. Feng, C.; Li, Z.; Shahidehpour, M.; Wen, F.; Li, Q. Stackelberg game based transactive pricing for optimal demand response in power distribution systems. *Int. J. Electr. Power Energy Syst.* **2020**, *118*, 105764. [CrossRef]
23. Zhang, Y.; Zhao, H.; Li, B.; Wang, X. Research on dynamic pricing and operation optimization strategy of integrated energy system based on Stackelberg game. *Int. J. Electr. Power Energy Syst.* **2022**, *143*, 108446. [CrossRef]
24. Wei, W.; Chen, Y.; Liu, F.; Mei, S.W.; Tian, F.; Zhang, X. Stackelberg game Based Retailer Pricing Scheme and EV Charging Management in Smart Residential Area. *Power Syst. Technol.* **2015**, *39*, 939–945.
25. Zhang, H.; Zhang, S.; Cheng, H.; Zhang, X.; Gu, Q. A State-of-the-Art Review on Stackelberg game and Its Applications in Power Market. *Trans. China Electrotech. Soc.* **2022**, *37*, 3250–3262.
26. Yang, S.; Tan, Z.; Zhou, J.; Xue, F.; Gao, H.; Lin, H.; Zhou, F.A. A two-level game optimal dispatching model for the park integrated energy system considering Stackelberg and cooperative games. *Int. J. Electr. Power Energy Syst.* **2021**, *130*, 106959. [CrossRef]
27. Zhang, P.; Zhang, B.; Yin, J.; Shi, J. County-Level Distributed PV Day-Ahead Power Prediction Based on Grey Correlation Analysis and Transformer-GCAN Model. *IEEE Trans. Sustain. Energy* **2026**, *17*, 709–717.
28. Jia, L.; Pang, X.; Wang, G.; Zhong, Y. A Day-Ahead Wind Power Forecasting Method Based on Physical Limitation Characteristics and Wind Speed Trend Clustering. In Proceedings of the 2025 6th International Conference on Electrical Technology and Automatic Control (ICETAC), Nanjing, China, 20–22 June 2025; pp. 161–164.
29. Sun, H.; Sun, X.; Kou, L.; Zhang, B.; Zhu, X. Optimal scheduling of park-level integrated energy system considering ladder-type carbon trading mechanism and flexible load. *Energy Rep.* **2023**, *9*, 3417–3430. [CrossRef]
30. Wang, L.; Dong, H.; Lin, J.; Zeng, M. Multi-objective optimal scheduling model with IGDT method of integrated energy system considering ladder-type carbon trading mechanism. *Int. J. Electr. Power Energy Syst.* **2022**, *143*, 108386.
31. Zhang, X.; Liu, X.; Zhong, J. Integrated Energy System Planning Considering a Reward and Punishment Ladder-type Carbon Trading and Electric-thermal Transfer Load Uncertainty. *Proc. CSEE* **2020**, *40*, 6132–6142.
32. Wu, Q.; Li, C. Modeling and operation optimization of hydrogen-based integrated energy system with refined power-to-gas and carbon-capture-storage technologies under carbon trading. *Energy* **2023**, *270*, 126832. [CrossRef]

Disclaimer/Publisher's Note: The statements, opinions and data contained in all publications are solely those of the individual author(s) and contributor(s) and not of MDPI and/or the editor(s). MDPI and/or the editor(s) disclaim responsibility for any injury to people or property resulting from any ideas, methods, instructions or products referred to in the content.